RF discharge at medium and high pressure & its possibilities for material surface modification

A.F.Alexandrov, G.E. Bugrov, E.A. Kralkina, V.B. Pavlov, V. Plaksin, V.P.Savinov, V.Yu. Sergeenko, I.B. Timofeev, K.V. Vavilin

Physical Faculty of Moscow State University, Russia, Moscow 119899GSP, Vorobievy gory

Introduction

During last years the tendency became evident to develop and utilize discharge at medium and high pressure in industry especially for plasma chemical applications and surface modification of materials. The review of the literature [1] devoted to this subjects, on the one hand specifies wide opportunities of such discharges and on the other hand demonstrates absence of detailed understanding of physical processes mechanisms in medium and high pressure discharges as well as mechanisms of its influence on material surface. The present paper represents the first results obtained in the field of systematic study of atmospheric RF discharge parameters together with results of discharge influence on material surface characteristics.

Discharge configuration and experimental procedure

Two types of discharge configuration were used in the experiments. The first one corresponds to pin-plane geometry. Its scheme is shown on Fig.1. The discharge was ignited between pin 1 and grounded metal plate 2 that were separated by the air gap with the length varied within the range 4-15mm. In some experiments the metal plate was covered by the dielectric layer 3. The additional gas flow was organized with the help of gas distributor 4. For ignition and sustaining of discharge RF generators 5 with the working frequency 0.6 MHz and 13.6MHz were connected to the electrodes 1 and 2 through the matching box 6.

The second type discharge being the prolonged one was generated with the help of the device schematically shown on Fig.2. The ignition electrode 1 helped to initiate discharge between metal string 1 and metal plate 2. The air flow having longitudinal and transversal components of velocity (in respect to the primary discharge) provided necessary homogeneity of the discharge.

In order to study discharge properties time dependencies of applied voltage and discharge current, volt-ampere characteristics and time averaged potential difference between plasma and electrodes were measured with the help of electrical scheme shown on Fig.3. The RF current and

RF voltage supplied to the discharge electrodes were measured with the help of current probe and RF voltage divider which signals were registered by computer equipped by RF ADC. The RF (V) and DC (U) voltage between points A, B, C were measured with the help of RF voltage divides and cathode voltmeters. The time averaged potential differences between plasma and electrode B U_{BE} was calculated using the formula:

$$U_{BE}=[V_{BC}/(V_{AB}C_{AB}-V_{BC}C_{BC})-U_{BC}/U_{CD}C_{CD}]$$
$$[1/U_{AB}C_{AB}+1/U_{CD}C_{CD}]. \qquad (1)$$

Alongside with electrical measurements the discharge radiation spectra, spatial radiation distribution were measured in dependence on discharge gap length, RF power, RF frequency and air flow rate. Gas temperature was measured on the basis of the rotational structure of the second positive band of nitrogen molecule.

In order to study the mechanism of the prolonged discharge formation video filming of discharge was carried out. As well the time correlation of 4 photodiodes signals assembled at different distances from the ignition electrode was studied (see Fig.4).

In order to study the possibility of RF atmospheric discharge utilization for materials surface modification the samples of different materials preliminary cleaned by ethyl alcohol were mounted on the plastic layer positioned on the grounded plate, then after ignition of the discharge samples were treated by plasma during their multiple scanning in respect to the string. After treatment the wettability of the samples was tested on the basis of contact angle measurements. In order to test adhesion the peel strength necessary for disassembling 3M scotch attached to the treated samples surface was measured.

Experimental Results

The volt-ampere characteristic of 13.6MHz pin-plate discharge is shown on Fig.5a. It is worth to note that in order to measure the VA curve the power of RF generator was increased step by step and corresponding values of RF voltage and current registered. The sections of VA characteristic corresponding to higher values of RF power are pointed by letters in ascending order starting from A.

The section AB of VA curve corresponds to the case when discharge is absent. After ignition of the discharge at the point B the discharge voltage reduces. The section CD corresponds to the conditions when the glowing part of the discharge originating near the pin does not touch the plate. In this case the discharge current is closed by the current of negative ions and displacement current. At the point D discharge touches the plate and the sheath between

plasma and electrode is created. The decrease of discharge RF voltage takes place in this point. The point F corresponds to the transition of discharge to arc. The RF current represented on Fig.5a is the total discharge current. Fig.5b illustrates the dependence of active part of discharge current on discharge voltage. One can see that after filling the space between pin and plate by plasma at the point D the increase of RF power results in the active current increase and discharge RF voltage decrease. Thus stable discharge mode with negative differential resistance was observed. Most probably the heating of the gas, contraction of the discharge channel and thermal electron emission of the pin contribute to the appearance of the said mode.

The potential difference between plasma and electrodes calculated in accordance with formulae (1) showed that the pin and plate have negative potential (about –100V and –10V correspondingly) in respect to plasma. Spectral measurements showed that in case if discharge is concentrated only near the pin the intensities of nitrogen molecule and molecular ion radiation are maximal near the pin and decrease monotonically with the increase of the distance from the pin. If discharge occupies the whole gap between pin and plate one can see the appearance of the second maximum of radiation near the plate (see Fig.6). The presence of dielectric layer between metal plate and discharge does not change qualitatively the observed situation. The appearance of the second radiation maximum can be evidently attributed to the formation of the sheath near the plate as well as near the pin. The presence of the sheath near the plate where the samples under treatment are to be located manifests that one of the important factors of sample treatment under atmospheric pressure is its irradiation by fast ions accelerated in the sheath similar to that in low pressure plasma.

The dependence of active discharge RF current on time is close to sinusoidal one. Only at the small length between pin and plate weak anharmonicity was observed (see Fig.7). The situation is quiet different if one uses 0.6MHz discharge. Even the appearance of 0.6MHz and 13.6MHz pin-pate discharges are quiet different, i.e. discharge at 0.6MHz has evident filamentary structure while discharge at 13.6MHz under relatively low air flow is flame one, no separate filaments can be seen.

Typical time dependencies of 0.6MHz discharge voltage and active current are shown on Fig.8, representing significant anharmonicity of active current. Under condition when pin has positive potential in respect to plate the breakdown of discharge gap takes place during every period of RF power.

The difference between 13.6MHz and 0.6MHz pin-plate discharges manifests itself in the way of the prolonged discharge formation. The results of video filming of 13.6MHz discharge is shown on Fig.9. One can see that first ignition of the flame in the vicinity of the ignition electrode takes place. Then due to the air flow the flame moves along the wire. After reaching

the end of the wire the discharge turns off and the new one is ignited with the help of ignition electrode. The increase of transversal gas velocity leads to the increase of the discharge repetition frequency. The results were confirmed in experiments with photodiodes distributed along the discharge. The time difference between current pulses of photodiodes were proportional to the distance between them and inversely proportional to the gas velocity.

The situation is different in case of 0.6MHz discharge with low air flowrate. One could see that signals of photodiodes were randomly distributed in time. That means that discharge areas are distributed randomly along the string and do not change their position due to gas flow. The lifetime of each microdischarge is about 10-20 msec, after its disappearance the new one appears at different point of the string. The increase of RF power leads to the simultaneous existence of several microdischarges. Significant increase of the air flow brings the mechanism of 0.6MHz prolonged discharge formation to that typical for 13.6MHz one.

The measurements of averaged in time intensity of discharge radiation showed high homogeneity of the prolonged RF discharge in all mentioned modes of its maintenance (see Fig.10). The increase of the gas flow leads to the homogenizing of the discharge radiation in the gap between electrodes. The same trend is typical for gas temperature (see Fig.11).

Improvement of PTFE adhesion in air discharge at atmospheric pressure was carried out in RF discharges with working frequencies 0.6 and 13.6MHz.

The results obtained with 13.6MHz discharge treatment of PTFE are represented at Fig.12,13. One can see that adhesion improvement of PTFE is possible but very large number of scannings is necessary. The number of scannings can be reduced by increasing the air flowrate, i.e. by increasing the speed of running flame and decreasing the speed of sample movement. Surface analysis of the treated samples showed that high deficiency of fluorine leading to adhesion improvement takes place on the surface but surface treatment is very inhomogeneous.

In order to improve the situation the 0.6MHz discharge with very small air flowrate was used. The obtained results are represented on Fig. 14. One can see that the number of treatments is reduced and adhesion strength is increased. Unfortunately due to the drawbacks of construction of line drive system small line drive velocities are impossible. One can see from Fig.14 that substantial adhesion improvement took place.

Experiments showed that as a result of samples processing in the discharge the wetting angle of the PTFE, PE, PI and vinyl chloride decreased until 40^{o}, 20^{o} ,25^{o} correspondingly, adhesion of PTFE being 4 times improved, the wetting angle of Al, SUS and carbon steel decreased until $10\text{-}20^{o}$. The treatment of samples was uniform due to homogeneity of discharge.

References

[1]. Proceedings of HAKONE YII Conference.

Greifswald, 2000.

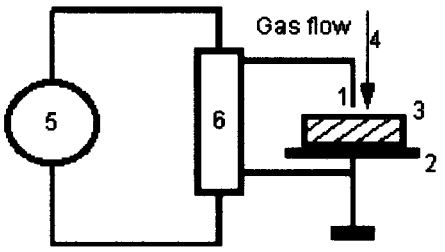

Fig1. The sceme of pin-plate experiment 1–pin, 2–plate, 3–sample, 4–gas distributor, 5 –RF generator, 6-matching box

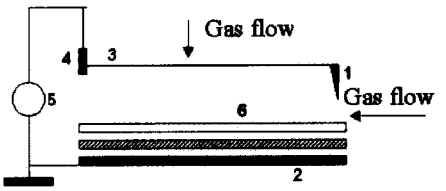

Fig 2. The sceme of string-plate experiment. 1–ignition electrode, 2–plate, 3,4 –working and feeding electrodes, 5–RF generator, 6-sample

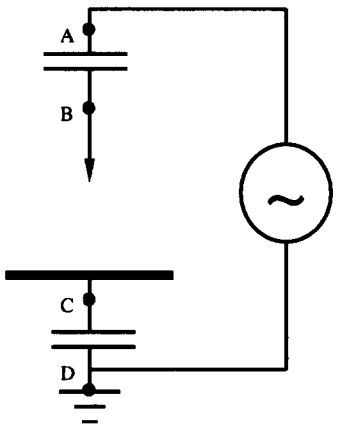

Fig.3. the sceme of electric measurements

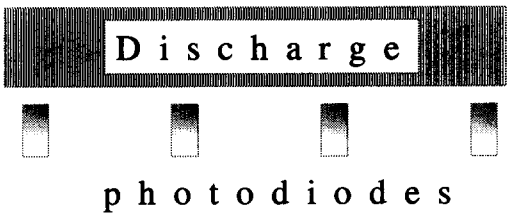

Fig.4. The scheme of experiment with photodiodes

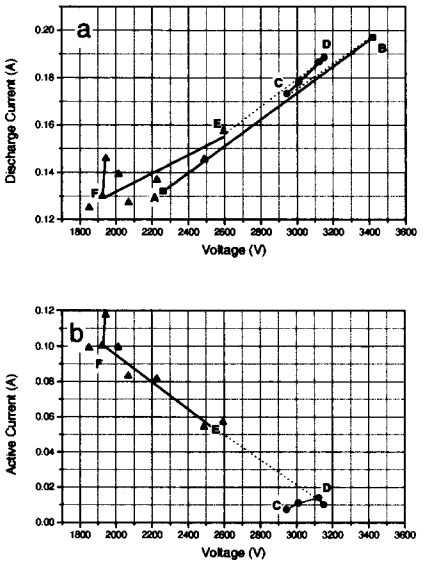

Fig5. VAcharacteristics of 13.6MHz pin-plate discharge

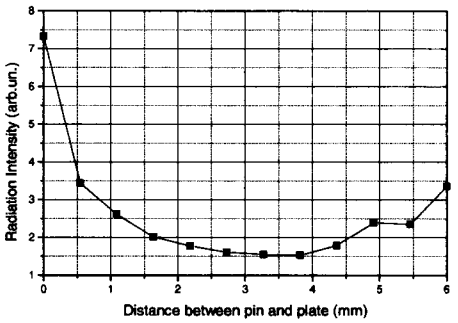

Fig.6. Dependence of discharge radiation intensity on the distance from pin

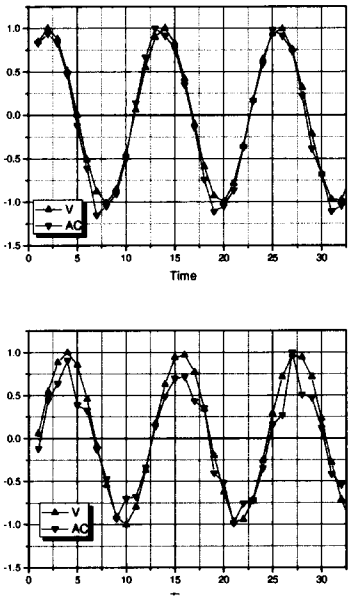

Fig.7. Ocsillograms of active current. 13.6MHz discharge, a- discharge length 15mm, b – 5mm

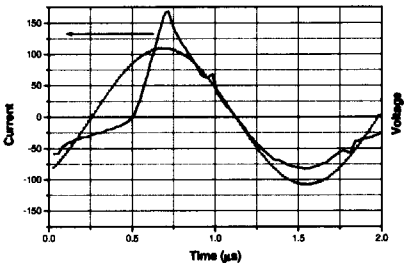

Fig.8. Oscillogram of active Current. 0.6MHz discharge.

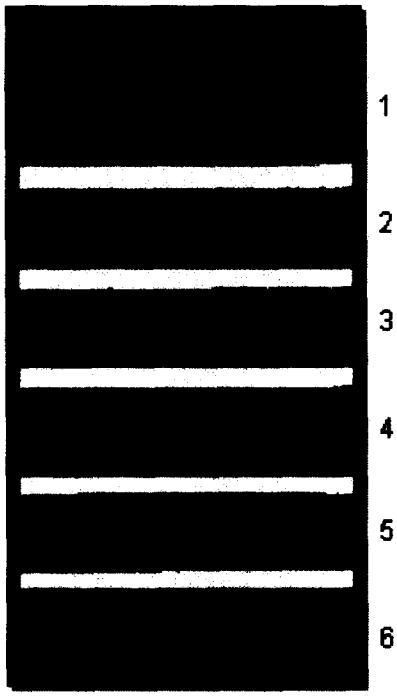

Fig.9. The video filming of 13.6MHя discharge. The time difference between pictures is 40mc.

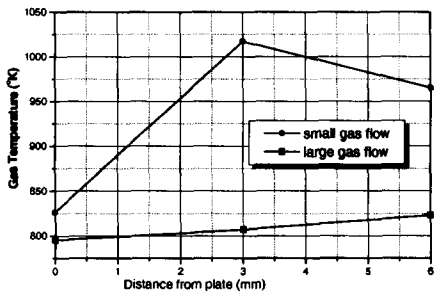

Fig10. Dependence of gas temperature on distance from plate

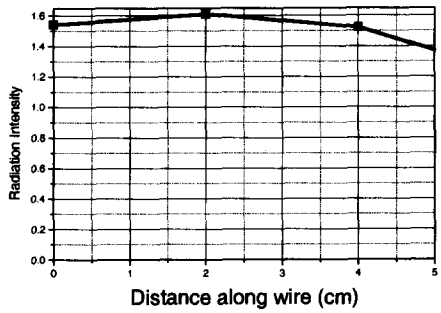

Fig.11. Longitudinal dependence of radiation intensity

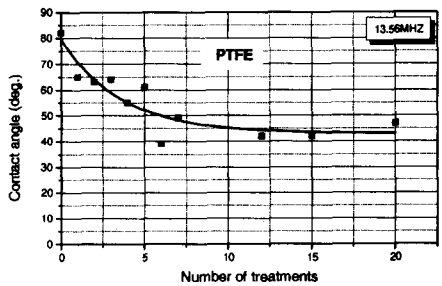

Fig.12. Dependence of PTFE contact angle of scannings number. 13.6MHz discharge

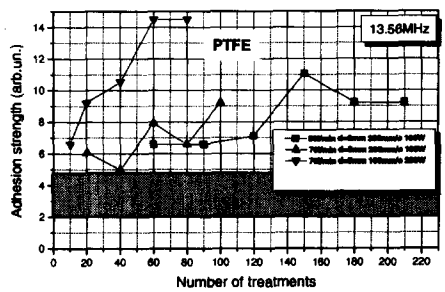

Fig.13. Dependence of PTFE samples adhesion strength on treatment number. 13.56MHz discharge. Gray bar marks the corridor where the adhesion strength values of non-treated PTPE samples are distributed.

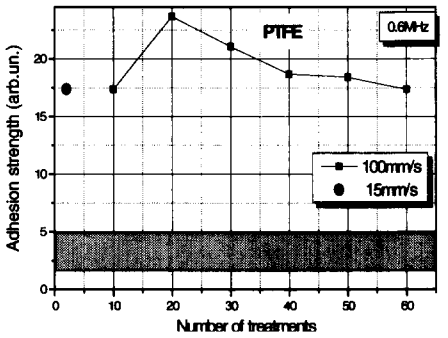

Fig.14. Dependence of PTFE samples adhesion strength on treatment number. 0.6MHz discharge. Gray bar marks the corridor where the adhesion strength values of non-treated PTPE samples are distributed.